Optimization of a Cabin Structure Considering the Water-Entry Process

HE Ziyi[1], *WANG Chen*[1*], *HU Qi*[2], *DONG Songwen*[2], *ZHANG Yu*[1], *SHEN Xing*[1], *ZHANG Jun*[1]

1. College of Aerospace Engineering, Nanjing University of Aeronautics and Astronautics, Nanjing 210016, P. R. China;
2. China Special Vehicle Research Institute, Jingmen 448035, P. R. China

(Received 14 March 2024; revised 8 May 2024; accepted 10 June 2024)

Abstract: The cabin structure of amphibious aircraft needs to withstand the impact force in the process of water-entry, which will affect the performance of amphibious aircraft significantly. A baseline cabin structure for an amphibious aircraft is established. According to the cabin geometry, the pressure distribution on the cabin during the water-entry process is obtained by numerical simulation. A finite element model of the cabin structure is established and the parametric study is carried out to obtain the effects of different design parameters on the cabin structure. Then, a framework is built to optimize the cabin structure, with the structural deformation and stress distribution during the water-entry process taken into account. In the optimization, the strain and stress are regarded as the constraints and the structure mass is the objective. After the optimization, the optimized design is further verified using the one-way coupling analysis method. The results show that the distribution of internal stringers and the thickness of the bottom skin have a significant influence on the maximum von Mises stress. By optimizing the design parameters of the cabin structure, the structure mass can be significantly reduced while the structural strength and stiffness can satisfy the constraints simultaneously.

Key words: cabin structure; amphibious aircraft; fluid-structure interaction; water-entry; structural optimization

CLC number: V212 **Document code:** A **Article ID:** 1005-1120(2024)03-0359-13

0 Introduction

Amphibious aircraft, which can take off and land on both water and land, play a key role in a variety of missions, such as emergency response and rescue. A complex fluid-structure interaction phenomenon will occur when the amphibious aircraft takes off or lands on the water. Different from conventional aircraft, the amphibious aircraft needs to withstand the short-term but strong hydrodynamic load, which becomes one of the primary loads in the structural design of amphibious aircraft[1]. The cabin structure is an essential part of the amphibious aircraft, which needs to carry the weight of the onboard equipment and resist the impact force while landing on the water. To ensure the safety, the cabin structure weight could account for a high fraction of the overall structure weight. Thus, how to design a lightweight cabin while meeting its load-carrying requirements has become a significant problem in the development of amphibious aircraft.

The cabin structure of amphibious aircraft needs to consider the hydrodynamic load during landing. This process can be simplified as a water-entry problem, and numerous studies have been performed in this field. Dated back to 1920s, Von Karman[2] has carried out study on the water-entry impact of structures by using the additional mass algorithm method. The floating raft structure of an amphibious aircraft was simplified as a two-dimensional wedge, and the pressure load formula of the collision between an amphibious aircraft and the water

*Corresponding author, E-mail address: cwangaero@nuaa.edu.cn.

How to cite this article: HE Ziyi, WANG Chen, HU Qi, et al. Optimization of a cabin structure considering the water-entry process[J]. Transactions of Nanjing University of Aeronautics and Astronautics, 2024, 41(3): 359-371.

http://dx.doi.org/10.16356/j.1005-1120.2024.03.008

surface was deduced according to the law of conservation of momentum. Wagner[3] proposed the approximate blunt flat plate theory with a small inclination model to solve the overall force on the structure during its entry into the water. Also, considering the liquid surface has a bulging phenomenon, the lifting of the liquid surface during impact was regarded as the liquid's around-flow motion on the flat plate. Vitaly et al.[4] found that amphibious aircraft had a reduced flight performance compared with land-based aircraft of the same size due to the presence of bottom hulls or pontoon structures. Bahulekar[5] studied splash bars on the bottom of a ship, and the results showed that they could effectively improve the take-off and landing performance of the hull, and help to reduce the splash.

Experimental study was also performed in this field. In 1940s, the National Advisory Committee for Aeronautics (NACA) firstly conducted experimental research on the water landing performance of aircraft. Steiner[6] established the dynamic models of B-26, B-25, B-17F, B-24 and A-20A, and carried out the water landing experiment of the aircraft, which provided a reference for the rescue work of aircraft landing on water. Tveitnes et al.[7] conducted water entry tests on wedge to investigate the effects of mass, angle, and velocity on the surface pressure of the structures. Panciroli et al.[8-9] studied the water-entry process of the wedge-shaped structure, and analyzed the fluid-structure coupling phenomenon of elastic structures during the water-entry process. The dynamic response of the structures was examined and it was found that the larger structural deformation has an important effect on the flow of fluids. Sun et al.[10] investigated the relationship between acceleration and strain during the water-entry process and the structural response law of wedges in the water entry process by changing the conditions of wedges with different oblique inclination angles, velocity, thickness and other parameters. Canamar[11] carried out an experimental study on the take-off characteristics of different bottom shapes under different sea conditions, which provided a certain basis for the design of amphibious aircraft's cabin. Wang et al.[12] took experimental and numerical simulation methods to study the pressure on the bottom and top of the wedge during free-falling dropping into the water.

Considering the experimental cost, numerical study has become more and more important. In the 1990s, Ghaffari[13] used boundary element and panel methods to simulate the air and water bypassing flow in the vicinity of the aircraft profile and analyzed the aerodynamic and hydrodynamic loads of the forced landing of the space shuttle at an attitude angle of 12° on water based on the linear potential wave theory. Hu et al.[14] established a finite element model for a certain type of airplane and predicted the pressure distribution of the fuselage by carrying out the water landing tests. Based on Froude's similarity criterion, the pressure distribution was applied to the finite element model to verify the water landing performance of the fuselage. Liu et al.[15] used the commercial software to conduct simulation analysis and structural optimization of the landing performance of an amphibious aircraft, as well as transient analysis of the structure based on the optimization results, which provided an engineering reference for the design of amphibious aircraft. Lü et al.[16] used a numerical simulation method to analyze the mechanical response of an amphibious aircraft during takeoff, landing, and encountering sudden winds, and the structural strength of the local area of the fuselage was redesigned and checked. Sun et al.[17] analyzed the structural response and load characteristics of a cylinder entering the water at high speed by using the fluid-structure interaction, and the results showed that considering the fluid-structure interaction effect, structural deformation would occur when the cylinder entered the water at high speed, and at the same time, the impact pressure appeared obvious fluctuation characteristics on the surface. Li et al.[18] solved the non-constant Reynolds-averaged Navier-Stokes (RANS) equation and k-ε turbulence model based on the finite volume method in an absolute coordinate system to simulate the aerodynamic characteristics of a large amphibious aircraft flying in the wave-surface ground effect region. Yan et al.[19] proposed a fluid-structure interaction modeling method that could be used to pre-

dict the inlet thumps of a flat plate and a wedge, and respectively compared them with the experimental results. Li et al.[20] studied the effect of the fluid-structure coupling on the impact load, the results showed that the greater the velocity of water entry, the greater the effect of liquid compressibility on the impact load of water entry, and at the same time, considering the compressibility, the evolution of the field of the water entry changed. Li et al.[21] studied the waterborne forced landing performance of civil aircraft under wave conditions and conducted a numerical simulation of civil aircraft waterborne forced landing to compare the process of aircraft waterborne forced landing under static water and wave water.

It can be seen quite a few studies have been performed to investigate the water-entry problem theoretically, numerically and experimentally. However, most of the previous studies focus on load characteristics and structural response analysis in the process of water entry and few optimizations of the cabin structural design have been performed. The effects of different design parameters of the cabin structure have not been fully investigated and the contributions of different cabin structural components during the water-entry process have not been fully understood.

This paper will firstly propose a typical cabin structure of the amphibious aircraft as a baseline design. And the landing process of the amphibious aircraft cabin is modeled as a hydrodynamic impact problem. The volume of fluid wave is adopted together with the Euler multiphase flow model to numerically simulate the hydrodynamic characteristics of the water-entry problem. Additionally, in the current study, the comparison of the one-way and two-way coupling scheme is also conducted to ensure that the selected numerical method is proper. Then, finite element models are established for parametric study and the effects of different design parameters on the cabin structure are investigated. Finally, genetic algorithm is used to optimize the cabin structure with the von Mises stress and strain in the cabin structure taken as constraints.

1 Model Definition and Numerical Methods

1.1 Model definition

The geometry of the cabin structure of a typical amphibious aircraft is illustrated in Fig.1, in which the main parameters are shown in Table 1. The main structures of the cabin include the skin, the bulkhead, the tip bearing structure, and the bottom stringers.

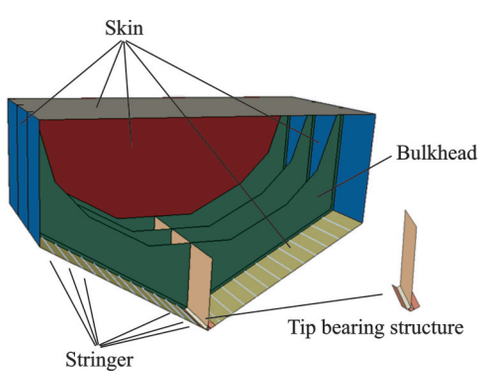

Fig.1 Cabin model

Table 1 Design parameters of the cabin structure

Parameter	Baseline value	Parameter	Baseline value
Length/m	3.25	Top skin thickness/mm	6
Height/m	1.988	Left and right side skin thicknesses/mm	1.6
Width/m	1.5	Front and rear side skin thicknesses/mm	1.6
Number of the stringer	12	Bottom skin thickness/mm	1.27
Volume/m^3	0.090 4	Thickness of bulkhead /mm	4
Bottom thickness of tip bearing structure/mm	3.5	Vertical thickness of tip bearing structure/mm	3.5
Mass/kg	709.6	Material	Steel

1.2 Numerical modeling of the water-entry process

With the geometry defined in the above section, the impact force on the cabin structure can be obtained by solving the water-entry process of the cabin model. In this paper, the commercial software

STAR-CCM+ ® (17.02.007)[22] is used to establish the water-entry model to get the hydrodynamic load. As shown in Fig.2, the computational domain is selected as a rectangular domain, and the background domain is set to be 15 m long, 5 m wide and 12 m high. The overset grid method is used to simulate the water-entry process. To obtain the changes in the gas-liquid interface and the pressure distribution during the water-entry process accurately, mesh refinement is performed on the gas-liquid interface. The total number of mesh is 2 733 120 and the mesh type is trimmed mesh. The VOF (Volume of fluid) wave is adopted to simulate the static water surface and Eulerian multiphase flow is selected, in which water is the main phase and the air is the secondary phase. As for the time model, an implicit unsteady state with constant time step is selected. RANS equations are used, and the turbulence model is selected as k-ε turbulence[23]. The background domain is fixed and the cabin structure motion is specified as translation. To avoid the reflection of shock waves, which might cause the coupling between the reflected waves and the cabin, symmetric boundary conditions are adopted around the background domain.

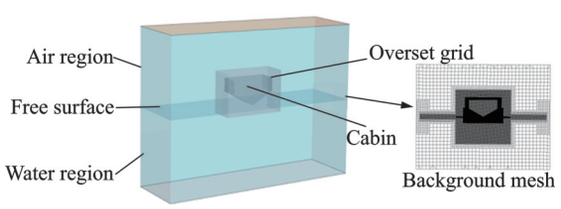

Fig.2 Computational domain schematic diagram and mesh refinement

1.3 Validation of the numerical method

The modeling method is firstly validated before further analysis is performed.

Using the same modeling method, the water-entry problem of a wedge-shaped model is created and compared with the results from the Refs. [24-25]. The height and width of the computational domain are 2 000 and 2 500 mm, respectively, heights of the air region and water region are 700 and 1 300 mm, respectively, and the total number of mesh is 449 786.

The shape of the wedge is an equilateral triangle, the top edge length of the wedge is 500 mm, the angle of inclined rise is 30°, the mass is set to 241 kg, and the velocity of water entry is 6.15 m/s. The velocity change is calculated and compared with the results from the Refs.[24-25] as shown in Fig.3.

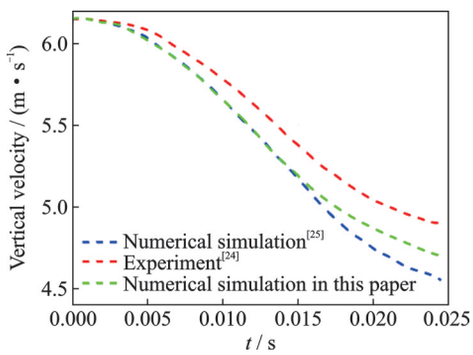

Fig.3 Comparison of velocity changes

The results from references and the proposed method have similar trends. In the early stage of the water entry, the numerical simulation and experimental results have a high degree of coincidence. With the increase of the water-entry depth, the velocity obtained by the numerical simulation method decays faster compared with the experimental results. Compared with the experimental results, the maximum error of the numerical simulation used in this paper is less than 5%, which indicates the feasibility of the proposed method.

The deformation of the multiphase flow interface and the morphology change of the jet during the water-entry process are also investigated. The obtained phase diagrams are compared with the experimental results to verify the simulation modeling method[25]. At the initial moment, the water surface is in contact with the tip split of the wedge, and the water entry velocity of the wedge is set to be 1 m/s.

Two different moments of the diagrams are shown in Fig.4, where the left side is the experimental results and the right side is the calculation results of the simulation analysis[25]. At 0.05 s, the free liquid surface is deformed to both sides due to the interaction with the wedge, and a high-velocity jet is generated. At 0.136 s, the free surface defor-

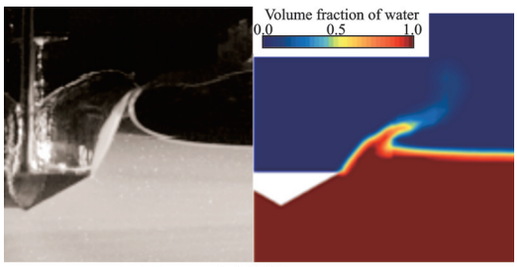

(a) 0.05 s

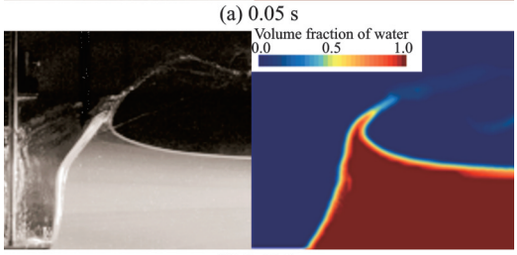

(b) 0.136 s

Fig.4 Comparison of the phase diagrams between experiment (Left) and simulation (Right) at different time[25]

mation increases and the high-speed jet is more obvious. With the increase of the water-entry depth, the free liquid surface above begins to converge to the center, which is close to the vertical direction at this time.

To quantitatively analyze the accuracy of the numerical simulation method used, the dimensionless parameters α and β are defined as follows

$$\begin{cases} \alpha = c_0/c \\ \beta = h_0/h \end{cases} \tag{1}$$

where c_0 is the distance between the highest point of the free liquid surface and the central axis of the wedge model in the horizontal direction, c half the length from the upper surface to the wedge, h_0 the distance between the highest point of the free liquid level and the upper surface of the wedge model in the vertical direction, and h the distance from the upper surface of the wedge to the bottom tip split; c and h are the fixed values. Fig.5 shows the details of c_0 and h_0 in the above expression. Table 2 shows the

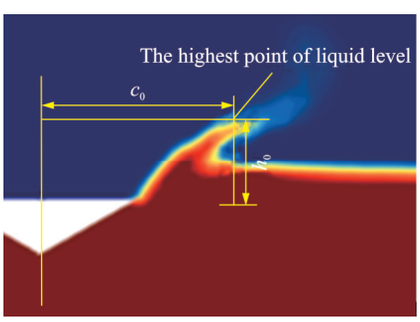

Fig.5 Details of c_0 and h_0

Table 2 Comparison simulation analysis and experimental results

Time/s	α			β		
	Simulation	Reference	Error/%	Simulation	Reference	Error/%
0.05	1.846	1.692	9.11	1.94	2.12	8.49
0.136	2.889	2.556	13.02	4.95	5.23	5.35

error between the numerical simulation and the experimental results in comparison with parameters α and β.

Compared with the diagrams and the dimensionless parameters, the jet profile from the numerical simulation can match the shape of the experimental results. The error can be the boundary condition. The pool used in the experiment is not infinite and there may be a wall reflection effect, while the CFD method uses the boundary condition of the symmetric plane to simulate the infinite water.

According to the results of the velocity change and the phase diagram, it can be concluded that the proposed numerical method can be used to simulate the water-entry process of the wedge-like model, such as the cabin model defined in the current study.

2 Parametric Modeling and Analysis of Cabin

2.1 Structural modeling

Considering the subsequent parameter analysis and structural optimization of the cabin structure, parametric model of the cabin structure is required. In this paper, a parametric finite element model of the cabin is established by commercial software Abaqus® and Python language, and the parameterization of the cabin structure can be used to quickly modify the parameters of the cabin structure to obtain different structural layouts. The cabin structure enters the water at a constant speed of 5 m/s. The hydrodynamic loads during the water-entry process are calculated by STAR-CCM+, which is used to parametric modeling and parametric analysis and optimization. For the cabin structure, the bottom skin is mainly subjected to in-plane load, and the stringer is mainly subjected to bending loads in the strengthening direction. The partition frame is mainly used

to maintain the cross-section shape and bear the local load of the skin in the cabin structure. The tip bearing structure is the first part to be subjected to hydrodynamic loads during the water-entry process, which is the main load-bearing component. Therefore, the number of bottom stringers N_1, the thickness of bulkhead T_1, the thickness of bottom skin T_2, the bottom thickness of tip bearing structure T_3, and the vertical thickness of tip bearing structure T_4 are selected as the optimization parameters, which are shown in Fig.6. For the above structure, the size of the thickness direction is much smaller than those of the remaining two directions. To simplify the calculation, reduce the time, and better reflect the actual structure's stress characteristics, the "beam-shell" unit is used to simplify the cabin structure under the premise of guaranteeing the accuracy of the calculation. In terms of element type, the beam element is selected as B31, and the shell elements are selected as S4R and S3. The mesh size is 30 mm, and the total number of mesh is 37 286. The cabin structure is made of high-strength low-alloy (HSLA) steel. HSLA steel is an alloy steel that has better mechanical properties or greater corrosion resistance than carbon steel. The parameters of high-strength low-alloy steel are set in the material library, as shown in Table 3.

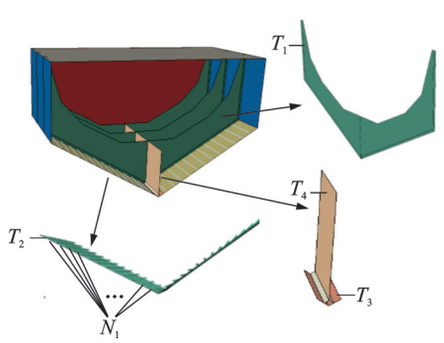

Fig.6 Schematic diagram of optimized parameters

Table 3 Property parameters of high-strength low-alloy steel

Modulus/MPa	Poisson's ratio	Tensile strength/MPa	Yield strength/MPa	Density/(t•mm^{-3})
210 000	0.3	470—630	355	7.85e−9

For the selection of the simulation time step, to ensure the accuracy of the calculation and save the computational resources, the time step is set to be 0.005 s, and the comparison effect of the maximum von Mises stress at different moments is shown in Fig.7. From the simulation results, it can be seen that compared with the minimum time step of 0.000 5 s, increasing the time step has a lower impact on the calculation results, and the error of the maximum von Mises stress in the moments shown in the figure is less than 5%. Considering that a safety factor will be assigned to ensure the stability of the cabin structure in the subsequent optimization process, the maximum von Mises stress error caused by the reduced time step is negligible.

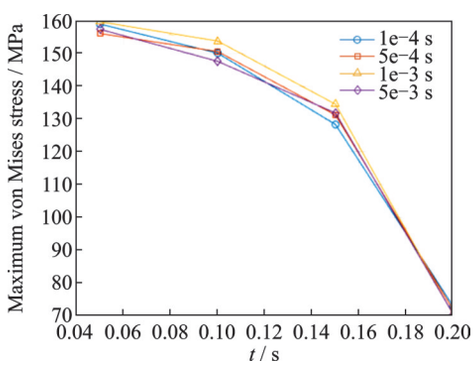

Fig.7 Stress comparison of different time steps

2.2 Selection of the coupling approach

With the numerical modeling method selected, the next water-entry of the cabin structure is a fluid-structure interaction process, during which the interaction between the cabin model and the fluid occurs. In this process, the cabin structure will be deformed due to the hydrodynamic load, and the deformation will affect the flow field, which changes the distribution of the hydrodynamic load in turn.

With the continuous development of computational mechanics and computer hardware capabilities, numerical simulation method has become an indispensable means in the study of fluid-structure interaction. There are basically two coupling approaches for the fluid-structure interaction analysis: One-way coupling and two-way coupling according to the way of data transmission. The one-way coupling is usually adopted when the structure deformation is not large and the corresponding change of the

fluid domain is small, which will almost not affect the distribution of the fluid loads.

In the one-way coupling approach, the fluid loads will be calculated first based on the initial geometry of the structure, after which fluid loads will be transferred onto the structure. The structure deformation will be checked to determine whether the change of the fluid domain is small enough for the one-way coupling. The advantage of the one-way coupling is that it is convenient for numerical simulation and requires low computational resources, but it cannot not fully capture the interaction between the fluid and structure. When the deformation of the structure is relatively large, a significant change will occur in the distribution of the fluid loads, which means the effect of the structure deformation is not negligible, and the two-way coupling is required in solving the problem.

In the two-way coupling approach, after the initial calculation, the geometry of the CFD model will be updated based on the structural deformation since the deformation of the structure is large enough. The updated CFD model will then be used to calculate the fluid loads, which will be transferred onto the structure model again. The subsequent calculation will follow the order until the structure deformation is small enough.

The basic steps of one-way coupling and two-way coupling are shown in Fig.8[26]. In this paper, the computational fluid dynamic software STAR-CCM+® and finite element software Abaqus® are used as the fluid and structure solver, respectively.

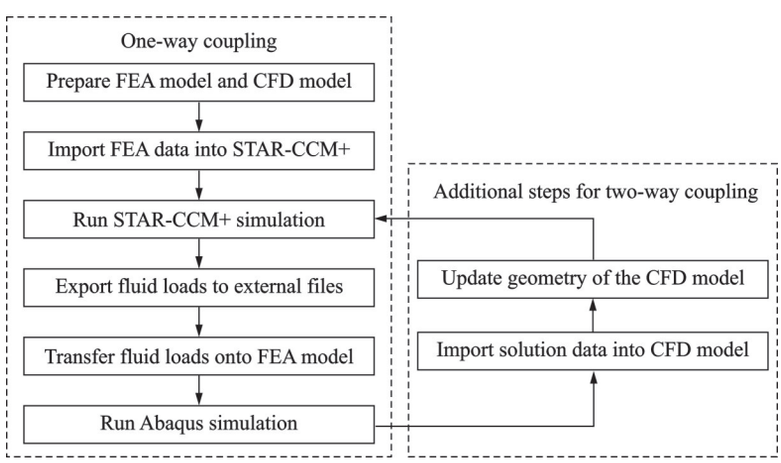

Fig.8 Flow chart of one-way and two-way coupling simulations of STAR-CCM+ and Abaqus[26]

To select a proper coupling approach, both the one-way and two-way coupling approaches are carried out and compared for the water-entry process of the cabin structure.

In the case study, the initial velocity of the cabin structure is 5 m/s, and 40 pressure monitoring points are set on the side of the cabin structure entering the water surface, as shown in Fig.9. In the one-way coupling approach, the entire water entry process (0.2 s) is divided into 40 stages, with each stage step running 0.005 s. The pressure distribution at 40 monitoring points is output as the load applied onto the structural model, which is analyzed in Abaqus. The loads and boundary conditions of the cabin structure are shown in Fig.9. In the two-way coupling, the finite element model is firstly established in Abaqus to export ".inp" file and the co-simulation command is added to it. It is necessary to set the path of the ".inp" file in the internal link of the STAR-CCM+ to achieve the data transmission. Due to the two-way coupling, the time step in the FEA model and CFD model should be consistent

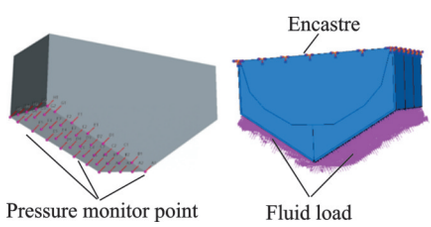

Fig.9 Pressure monitoring points and boundary condition of the cabin

which is set as 0.005 s, so as to ensure the real-time transmission of the data. For the mesh size, in order to ensure the accuracy of the data transmission, the mesh size of both should be as consistent as possible, which is set as 30 mm.

The structural behavior of the cabin is analyzed in Abaqus. The maximum von Mises stress for one-way coupling and two-way coupling are plotted using the Abaqus post-processing function, as shown in Figs.10 and 11.

From the results, it can be seen that the maximum von Mises stress of one-way coupling and two-way coupling structures are 114.6 MPa and 122.4 MPa, respectively, with an error of 6.3%. Fig.10 shows the maximum logarithmic strain of two-way coupling is $7.525e^{-4}$. For the cabin structure, since the material used is steel, and the water entry velocity is small. The deformation produced in the process of the impact of the cabin into the water is small as well, which does not have much influence on the change of the fluid domain, and the maximum von Mises stress produced by the one-way coupling and two-way coupling structures is not much different. For the calculation case, the two-way coupling takes about 10 h, while the one-way coupling takes only 5 min when using the same computing resources. Therefore, without loss of the calculation accuracy and considering the time cost required for the subsequent parameter analysis and structural optimization, the one-way coupling is chosen for the subsequent calculation and analysis.

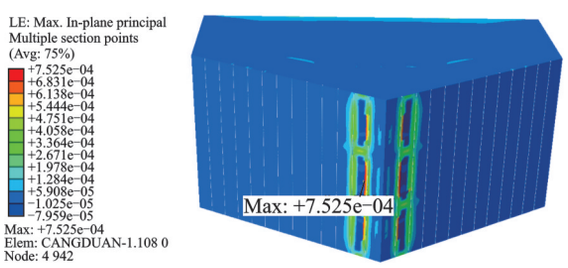

Fig.10 Strain cloud diagram of two-way coupling

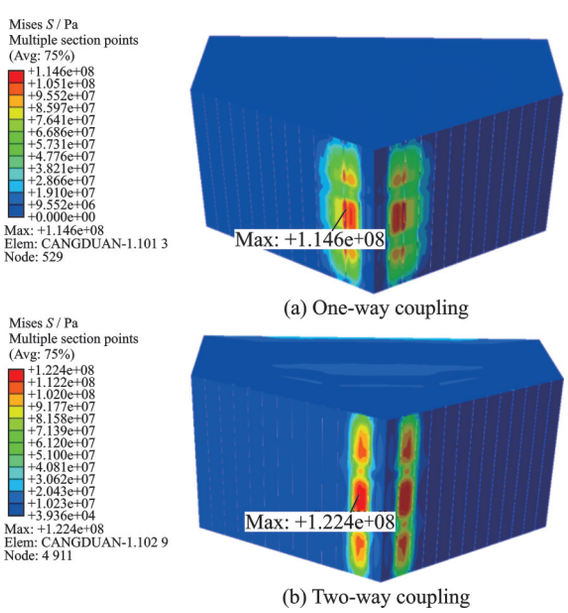

Fig.11 Stress cloud diagram of one-way and two-way couplings

2.3 Parametric study

To further investigate the relationship between the maximum stress, strain and the optimized parameters for the water-entry process of different layouts, parametric analysis is performed, and the results are shown in Figs.12—14.

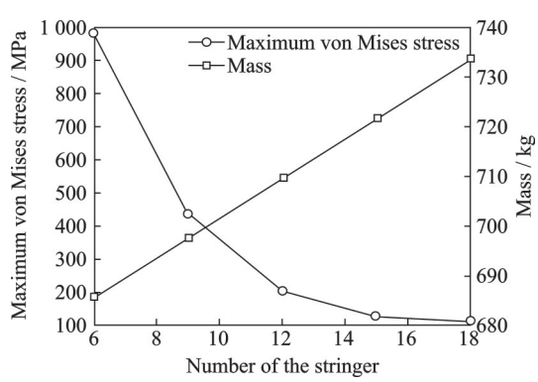

Fig.12 Influence of the number of the stringer on the maximum von Mises stress and mass of the structure

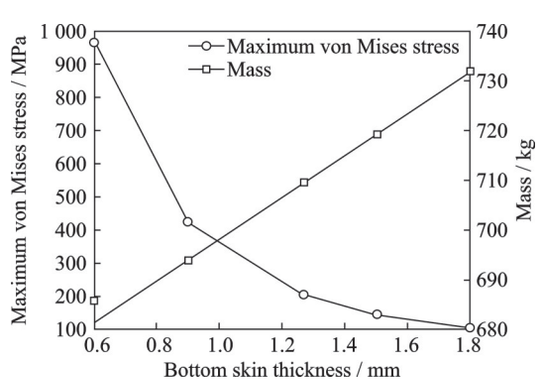

Fig.13 Influence of skin thickness on the maximum von Mises stress and mass of the structure

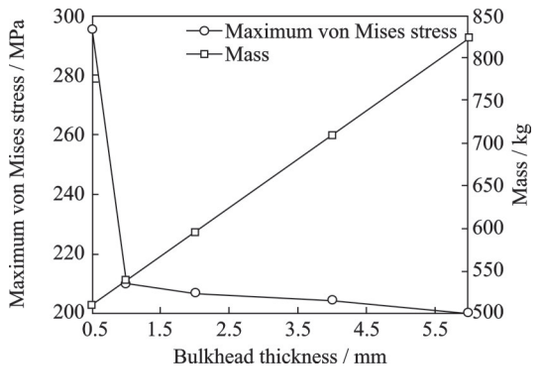

Fig.14 Influence of bulkhead on the maximum von Mises stress and mass of the structure

It can be seen that increasing the number of the stringer and the thickness of the bottom skin can significantly reduce the von Mises stress, but the increase in the number of the stringer and the thickness of the bottom skin will lead to an increase in the mass of the structure. For the number of the stringer, as shown in Fig.12, when the number of the stringer is less than 10, the maximum von Mises stress of the structure will exceed the allowable stress of the material and lead to the destruction of the structure, and with increasing the number of the stringer, the effect of reinforcement is not obvious when the number of the stringer is more than 15.

In terms of the thickness of the bottom skin, as shown in Fig.13, the reinforcing effect is similar to that of the stringer. In the case of the lower thickness of the structure, the strengthening effect is significant, but it gradually slows down with the increase in thickness.

The thickness of the bulkhead on the structural strengthening effect is shown in Fig.14. When the thickness is less than 1 mm, the bulkhead enhancement effect is more obvious; when the thickness is greater than 1 mm, the strengthening effect of thickness on the structure is limited, but the influence on the structure of the overall quality is very great.

It can be seen that the number of the stringer, the thickness of the bottom skin, and the thickness of the bulkhead are of great significance to the strength design of the cabin structure and the improvement of the structural economy based on the results of the above parameter analysis. For the tip bearing structure, the hydrodynamic load is borne by this part due to the first contact with the water surface during the water-entry process. It has a significant influence on the stability of the whole cabin structure, so it is necessary to optimize tip bearing structure and above structures to ensure the strength of the cabin structure.

3 Cabin Structure Optimization and Analysis

3.1 Establishment of optimization problem

According to the parametric study, the mass and the structural performance of the cabin structure can be further improved by tuning the parameters. To improve the flight performance of the amphibious aircraft, the cabin structure mass is taken as

$$G(x) = \min \text{Mass} \tag{2}$$

For the water-entry process, the distribution of the bottom stringer, the thickness of the bottom skin, the thickness of the bulkhead, the bottom thickness of tip bearing structure, and the vertical thickness of tip bearing structure are selected as optimization parameters. In addition, the optimization of the cabin needs to consider the maximum von Mises stress and strain in the process of water entry, which is specifically expressed as the tensile and compressive stress generated cannot exceed the allowable stress of the material, and the strain cannot exceed the allowable strain value. The cabin structure of amphibious aircraft is the main bearing part of the whole aircraft landing, so for the structural optimization, the safety factor is selected to be 1.5, that is, the maximum von Mises stress generated in the process of water entry is less than 237 MPa. Based on the above parameter analysis results, the upper and lower limits of each parameter for subsequent optimization are determined as shown in Table 4.

From the above three elements of optimization, an optimized mathematical model of the cabin structure as shown in the following equation is established.

Table 4 Initial value and upper and lower limits of design parameters

Parameter	Initial value	Lower value	Upper value
Number of the stringer N_1	12	9	18
Thickness of partition frame T_1/mm	4	0.2	5
Thickness of bottom skin T_2/mm	1.27	0.6	2
Bottom thickness of tip bearing structure T_3/mm	3.5	1	5
Vertical thickness of tip bearing structure T_4/mm	3.5	1	5

$$\begin{cases} G(\boldsymbol{x}) = \text{minMass} \\ \text{s.t.} \begin{cases} S_{\min} < S\_\text{all}\_\max \leqslant S_{\max} \\ E_{\min} < E\_\text{all}\_\max \leqslant E_{\max} \end{cases} \\ \boldsymbol{x} = [N_1, T_1, T_2, T_3, T_4]^{\mathrm{T}} \end{cases} \tag{3}$$

where $G(\boldsymbol{x})$ is the minimum structural mass of the cabin structure, and N_1, T_1, T_2, T_3, and T_4 are the five independent parameters for the optimization of the cabin structure, which represent the number of bottom stringer, thickness of the partition frame, thickness of the bottom skin, bottom and vertical thicknesses of the tip bearing structure, respectively. S is the von Mises stress in the dynamic analysis, S_all_max is the maximum von Mises stress, $S_{\min}$ and $S_{\max}$ are the upper limit and lower limit of the von Mises stress; E is the structural strain in the dynamic analysis, E_all_max is the maximum structural strain, $E_{\min}$ and $E_{\max}$ are the upper limit and lower limit of the structural strain.

In this paper, Abaqus® software[27] and MATLAB® genetic algorithm (GA)[28] are used to optimize the cabin structure. The specific optimization process is shown in Fig.15. Python scripts are used to modify the finite element model and read the finite element analysis results, and the data flow is controlled through MATLAB for the optimization. The maximum optimization generations are 50, which is a stopping criterion for the optimization process. Gene crossover probability is set as 0.8, which determines the proportion of individuals in the genetic algorithm that undergo gene crossover in each generation. The population size is 50, and the function convergence percentage is 0.01% in the optimization.

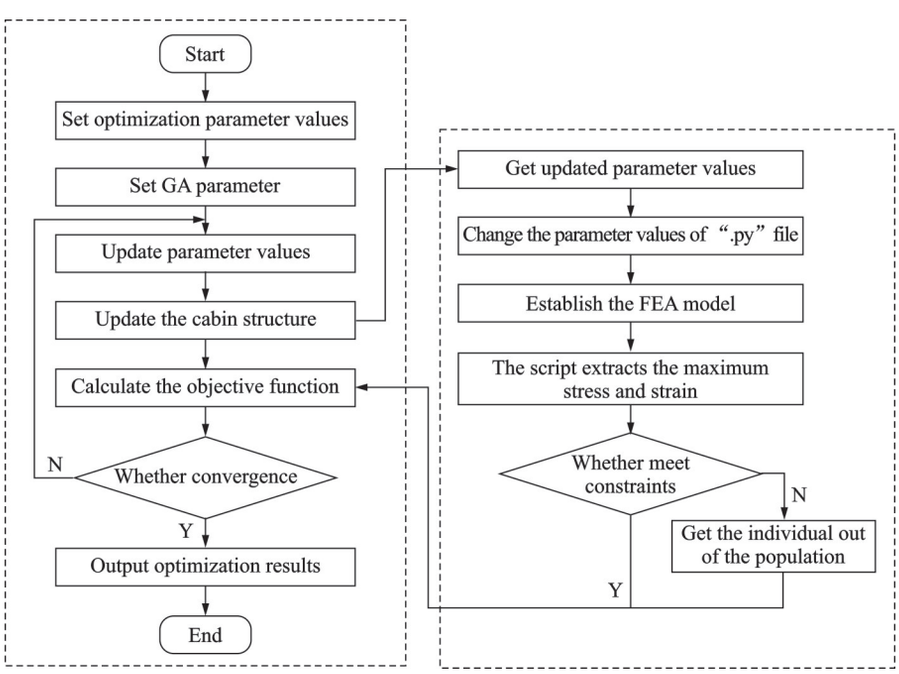

Fig.15 Optimization flow chart

3.2 Optimization process and result analysis

After the optimization iteration calculation, the optimization process of the cabin structure mass is obtained as shown in Fig.16, which shows a contin-

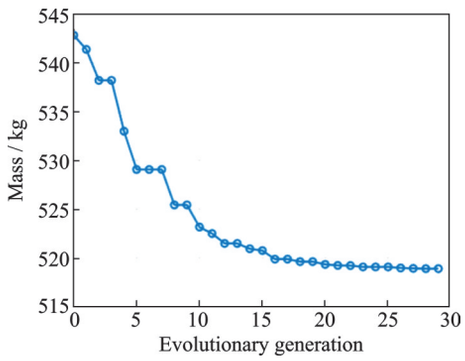

Fig.16 Diagram of cabin structure mass optimization process

uous decrease of the structure mass during the optimization process. From the figure, it can be seen that the cabin mass varies greatly in the initial iteration of the optimization process, and with continuous optimization, the curve gradually tends to be stable. In the 29th optimization iteration, since the percentage change of the cabin structural mass is smaller than the initial optimization setting, the optimization process is converged, the optimization is automatically terminated and the optimal value of the cabin mass of 518.9 kg is obtained, which is a 26.8% reduction in the structural mass of the cabin structure compared with the initial design (initial cabin mass is 709.6 kg).

The specific results of the design parameters obtained are shown in Table 5.

For the optimized layout of the cabin, the dynamic analysis of the cabin is carried out by using the same modeling approach, and the maximum von Mises stress and strain cloud diagrams of the optimized cabin are obtained as shown in Figs.17 and 18.

According to the dynamic analysis results of the optimized cabin layout, the maximum von Mises stress of the cabin structure is 234.1 MPa, and the maximum strain is $6.778e^{-4}$, which meets the requirements of the cabin design. The overall cabin structure mass decreases by 26.8%, which shows taking the strength and stiffness of the cabin structure as the constraints, it has a great potential of mass reduction of the cabin structure by changing the number of the stringer, the thicknesses of the bulkhead, tip bearing structure and bottom skin.

Table 5 Optimization results of design parameters

Parameter	Optimal value
Number of the stringers N_1	17
Thickness of partition frame T_1/mm	0.55
Thickness of bottom skin T_2/mm	0.92
Bottom thickness of tip bearing structure T_3/mm	1.94
Vertical thickness of tip bearing structure T_4/mm	2.97

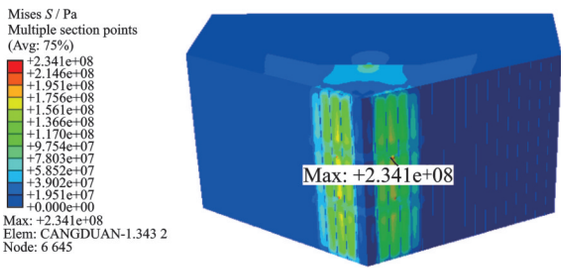

Fig.17 Stress cloud diagram of the optimized cabin structure

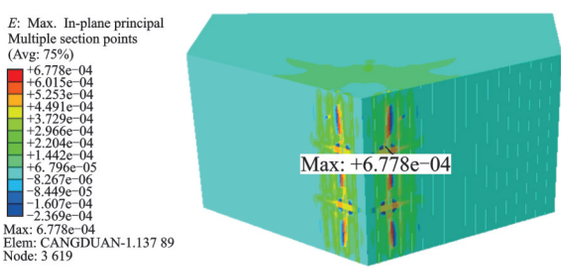

Fig.18 Strain cloud diagram of the optimized cabin structure

4 Conclusions

The numerical model of the cabin structure is established to investigate its structural performance during the water-entry process. The following conclusions can be summarized as:

(1) The one-way coupling approach is selected as the structural deformation is not high, which helps to perform the parametric study of the cabin structure. The parametric study shows the design variables of the cabin structure can be tuned to further reduce the structure mass while the structure constraints can be satisfied.

(2) A framework is created to optimize the cabin structure using generic algorithm. The optimization results show the structure mass can be reduced significantly while the maximum von Mises stress and strain can satisfy the constraints.

In the current study, the water-entry velocity is fixed since the focus is to perform the structural analysis and optimization. In the future study, the ef-

fects of the water-entry velocity on the structural deformation and the strength checking will be investigated using a two-way coupling approach to better represent the physics of the water-entry problem.

References

[1] SUN Feng, WEI Fei, WU Bin, et al. An experimental study on water impact of large amphibious aircraft[J]. Journal of Vibration and Shock, 2019, 38(12): 39-43. (in Chinese)

[2] VON KARMAN T. The impact of seaplane floats during landing: NACA Technical Notes 321[R]. Washington DC, USA: National Advisory Committee for Aeronautics, 1929.

[3] WAGNER H. Phenomena associated with impacts and sliding on liquid surfaces[J]. Journal of Applied Mathematics and Mechanics, 1932, 12(4): 193-215.

[4] VITALY Z, ALEXANDR M. Development trends of amphibian's shape[C]//Proceedings of the 29th Congress of the International Council of the Aeronautical Sciences (ICAS). St. Petersburg: ICAS, 2014.

[5] BAHULEKAR S S. Effect of spray rails on takeoff performance of amphibian aircraft[D]. Daytona Beach: Embry-Riddle Aeronautical University, 2022.

[6] STEINER M F. Ditching behavior of military airplanes as affected by ditching aids: NACA MR-L5A16 [R]. [S.l.]: NACA, 1945.

[7] TVEITNES T, FAIRLIE-CLARKE A C, VARYANI K. An experimental investigation into the constant velocity water entry of wedge-shaped sections[J]. Ocean Engineering, 2008, 35(2): 1463-1478.

[8] PANCIROLI R. Water entry of flexible wedges: Some issues on the FSI phenomena[J]. Applied Ocean Research, 2012, 39(1): 72-74.

[9] PANCIROLI R, ABRATEB S, MINAKA G, et al. Hydroelasticity in water-entry problems: Comparison between experimental and SPH results[J]. Composite Structures, 2012, 94(3): 532-539.

[10] SUN Hui, LU Zhihua, HE Yousheng. Experimental research on the fluid-structure interaction in water entry of 2D elastic wedge[J]. Journal of Hydrodynamics, 2003, 18(1): 104-109.(in Chinese)

[11] CANAMAR L, ALAN L. Seaplane conceptual design and sizing[D]. Glasgow: University of Glasgow, 2012.

[12] WANG J, LUGNI C, FALTINSEN O M. Experimental and numerical investigation of a freefall wedge vertically entering the water surface[J]. Applied Ocean Research, 2015, 51: 181-203.

[13] GHAFFARI F. Analytical method for the ditching analysis of an airborne vehicle[J]. Journal of Aircraft, 1990, 27: 312-319.

[14] HU Dayong, YANG Jialing, WANG Zanping, et al. Numerical model for a commercial aircraft water landing[J]. Journal of Beijing University of Aeronautics and Astronautics, 2008, 34(12): 1369-1374, 1383. (in Chinese)

[15] LIU Xiangyao, NIE Hong, ZHAN Jiali. Simulation for aircraft landing and structure optimization of amphibious aircraft[J]. Science Technology and Engineering, 2010, 10(30): 7611-7615.(in Chinese)

[16] LÜ Jihang, ZENG Yi, YANG Rong. Dynamic response characteristics of large amphibious aircraft[J]. Aeronautical Manufacturing Technique, 2020, 63 (20): 64-69.(in Chinese)

[17] SUN T, ZHOU L, YIN Z, et al. Cavitation bubble dynamics and structural loads of high-speed water entry of a cylinder using fluid-structure interaction method[J]. Applied Ocean Research, 2020, 101: 102285.

[18] LI Y H, FU X Q, CHEN J C. Numerical simulation of seaplane wave ground effect with crosswind[J]. Transactions of Nanjing University of Aeronautics and Astronautics, 2021, 38(S1): 1-9.

[19] YAN D N, HOSSEINZADEH S, LAKSHMYNARAYANANA A, et al. Comparative study on numerical hydroelastic analysis of impact-induced loads[C]// Proceedings of the 23rd Numerical Towing Tank Symposium. Mulheim An Der Ruhr, Germany: [s.n.], 2021.

[20] LI Guoliang, YOU Tianqing, KONG Decai. Effect of fluid compressibility on high-speed water-entry of revolutionary body[J]. Acta Armamentarii, 2020, 41(4): 720-729.(in Chinese)

[21] LI Meng, CHEN Xingyi, CHEN Jichang, et al. Numerical analysis of civil aircraft ditching performance in wave condition[J]. Acta Aeronautica et Astronautica Sinica, 2024, 45(2): 33-48. (in Chinese)

[22] STAR-CCM+ Inc. STAR-CCM+ user's guide[M]. [S.l.]:STAR-CCM+ Inc., 2022.

[23] YANG Q, TAN Z D, YU J C. Research on impact load of underwater glider entering water by airdrop[J]. Ship Science and Technology, 2023, 45(4): 67-73.

[24] ZHAO R, FALTINSEN O. Water entry of two-dimensional bodies[J]. Journal of Fluid Mechanics, 1993, 246: 593-612.

[25] CHEN Guangmao, ZHENG Xiaobo, WU Xiaoni, et al. Numerical and experimental study of water entry problem of two-dimensional wedge[J]. Ship Science

and Technology, 2021, 43(1): 53-60.(in Chinese)
[26] JIAO J, HUANG S, WANG S. A CFD-FEA two-way coupling method for predicting ship wave loads and hydroelastic responses[J]. Applied Ocean Research, 2021, 117: 102919.
[27] ABAQUS Inc. ABAQUS analysis user's guide[M]. [S.l.]: ABAQUS Inc., 2019.
[28] The MathWorks Inc. MATLAB R2020b. 2020[M]. [S.l.]: The MathWorks Inc., 2020.

Acknowledgements The work was supported by the National Natural Science Foundation of China (No.52305262) and the Starting Grant of Nanjing University of Aeronautics and Astronautics(No.1001-YQR22056).

Authors Mr. **HE Ziyi** received his B.S. degree in aircraft manufacture engineering from Nanchang Hangkong University in 2018. He is studying for a M.S. degree in mechanical engineering at Nanjing University of Aeronautics and Astronautics. His research interest is structural optimization.

Dr. **WANG Chen** received his Ph.D. degree in aerospace engineering in Swansea University. His research interests include smart structures and advanced aero-structures.

Author contributions Mr. **HE Ziyi** established the parameter model, built the optimization framework, conducted the analysis and wrote the manuscript. Dr. **WANG Chen** contributed to the overall planning and proofreading of the manuscript. Mr. **HU Qi** and Mr. **DONG Songwen** helped to query the domestic and foreign research status and performed the numerical verification. Mr. **ZHANG Yu** helped to calculate the hydrodynamic loads. Prof. **SHEN Xing** and Dr. **ZHANG Jun** helped to summarize the numerical methods and principles. All authors commented on the manuscript draft and approved the submission.

Competing interests The authors declare no competing interests.

(Production Editor: XU Chengting)

考虑入水冲击过程的舱段结构优化

何子懿[1], 王 晨[1], 胡 奇[2], 董松文[2], 张 雨[1], 沈 星[1], 张 军[1]
(1.南京航空航天大学航空学院,南京 210016,中国; 2.中国特种飞行器研究所,荆门 448035,中国)

摘要:水陆两栖飞机的舱段结构在入水过程中需要承受入水冲击力的作用,对水陆两栖飞机的结构性能有着重要影响。本文建立了水陆两栖飞机的初始舱段结构模型,基于该结构通过数值仿真方法获取了结构入水过程中的压强分布。建立了舱段结构的有限元模型并开展了参数分析,探究了不同设计参数对舱段结构的影响。在此基础上,考虑舱段入水过程中的结构变形与应力分布,搭建了舱段结构优化设计框架;以舱段结构的应力和应变作为约束、减少质量为目标开展优化设计;根据优化后得到的舱段结构,进一步验证了单向耦合分析方法的准确性。优化结果表明,舱段结构的底面加强筋分布以及底面蒙皮厚度对入水过程中结构产生的最大米塞斯应力有着重要影响。通过对舱段结构的设计参数开展优化设计,可以在满足强度与刚度的前提下,显著降低舱段结构的质量。

关键词:舱段结构;水陆两栖飞机;流固耦合;入水冲击;结构优化